Available online at www.sciencedirect.com
SCIENCE DIRECT®

Journal of the European Ceramic Society 24 (2004) 3049–3055

www.elsevier.com/locate/jeurceramsoc

Assessment of stability and protonic conduction in NASICON ceramics

R.O. Fuentes[a,b], O.A. Smirnova[a], V.V. Kharton[a], F.M. Figueiredo[a,c,*], F.M. Marques[a]

[a]*Department of Ceramics and Glass Engineering, CICECO, University of Aveiro, 3810-193 Aveiro, Portugal*
[b]*CINSO-CITEFA-CONICET, J.B. de la Salle 4397, B1603ALO Villa Martelli, Buenos Aires, Argentina*
[c]*Science and Technology Dep., Universidade Aberta, Roda Escola Politécnica 147, 1269-001 Lisbon, Portugal*

Received 23 May 2003; received in revised form 13 October 2003; accepted 25 October 2003

Abstract

NASICON-type $Na_3Si_2Zr_{1.88}Y_{0.12}PO_{11.94}$ and $Na_{3.2}Si_{2.2}Zr_{1.88}Y_{0.12}P_{0.8}O_{11.94}$ ceramics were obtained by a standard ceramic route. The structural and microstructural analysis of materials processed under different conditions suggested that the amount of Na- and P-rich liquid phases formed during the high temperature sintering is smaller for $Na_{3.2}Si_{2.2}Zr_{1.88}Y_{0.12}P_{0.8}O_{11.94}$. Indeed, samples of this composition showed a considerably worse sinterability. Total conductivity values obtained as a function of the humidity content show no evidence for protonic conduction in NASICON between 373 and 473 K. Results obtained at lower temperatures are not conclusive due to the significant degradation of the electrolyte/electrode interfaces and surfaces in wet atmospheres.
© 2003 Elsevier Ltd. All rights reserved.

Keywords: Conductivity; Impedance spectroscopy; Microstructure-final; NASICON; Powders–solid state reaction; Proton conduction

1. Introduction

After the first reports on fast sodium transport in $Na_{1+x}Zr_2Si_xP_{3-x}O_{12}$ solid solutions,[1,2] materials of this family called NASICON found important electrochemical applications, such as CO_2 sensors[3,4] and Na^+ ion-selective electrodes.[5,6] Na^+ conduction in NASICON is enabled by interstitials formed in a lattice consisting of ZrO_6 octahedra linked to SiO_4 or PO_4 tetrahedra by corner shared oxygens.[7] It has been known that the electrical performance of NASICON materials is severely compromised by their instability in contact with water, either liquid or vapour.[8–12] The first attempts to understand this problem, based on the study of powdered samples suspended in aqueous solutions, showed that the reaction occurs with Na^+ and PO_4^{3-} leaching from the NASICON whereas the pH of the solution increases.[8,9] This was interpreted as the result of the dissolution of Na_3PO_4 existing as a glassy phase at the grain boundaries and the incorporation of hydronium ions into the material leading to the formation of the so-called hydronium NASICON.[13] Later, an impedance spectroscopy study of dense NASICON ceramics previously exposed to water at 333 K confirmed that the reaction process is primarily located at the grain boundaries.[11] A large increase of the amplitude of the grain boundary impedance was observed for samples reacted for more than ca. 200 h whereas microstructural analysis revealed small grains of a second phase covering the NASICON grains. Complementary X-ray diffraction patterns collected on powdered samples suggested that the composition of these small grains is similar to that of hydronium NASICON. Although it is not known if the stability of NASICON varies with composition, results obtained with a humidity sensor based on P-free NASICON materials suggests that a higher Na:P ratio may lead to an improved stability of NASICON in contact with water.[14]

The fully hydronium-exchanged NASICON is known to be a fairly good protonic conductor.[12] The facility to which the ionic exchange between Na^+ and hydronium ions can occur drew our attention to the possible existence of protonic conduction in NASICON, albeit the possible degradation of the material. These are the central themes of the present study.

* Corresponding author. Tel.: +351-234-370263; fax: +351-234-425300.
E-mail address: framos@cv.ua.pt (F.M. Figueiredo).

0955-2219/$ - see front matter © 2003 Elsevier Ltd. All rights reserved.
doi:10.1016/j.jeurceramsoc.2003.10.040

2. Experimental

Nominal $Na_3Si_2Zr_{1.88}Y_{0.12}PO_{11.94}$ (NTZP20) and $Na_{3.2}Si_{2.2}Zr_{1.88}Y_{0.12}P_{0.8}O_{11.94}$ (NTZP22) NASICON-type compounds were prepared by solid state reaction of $(ZrO_2)_{0.97}(Y_2O_3)_{0.03}$ (Tosoh), $Na_3PO_4{\cdot}12H_2O$ (Merck), $Na_2CO_3{\cdot}10H_2O$ (Merck) and SiO_2 (Merck) as starting materials. The powder mixtures were ball-milled in ethanol, dried, and calcined in air at 1393 K (NTZP20) and 1453 K (NTZP22) for 8 h in a closed Pt crucible. After a second ball-milling step, the powders were isostatically pressed (200 MPa) into disks and then sintered. The sintering conditions and abbreviations used in this work are listed in Table 1.

Phase composition and lattice parameters of the synthesized powders and dense ceramics were determined by X-ray diffraction (XRD) using a Rigaku Geigerflex instrument (CuK_α radiation, step 0.01°, 5 s/step). The microstructure of the ceramics, polished and then thermally etched at 1373 K for 0.5 h, was evaluated by scanning electron microscopy (SEM). It is noteworthy that a detailed study of the nature and composition of grain boundaries (e.g. by transmission electron microscopy) failed due to the instability of the material under the beam.

The electrical properties of ceramic samples were characterised by impedance spectroscopy using a Hewlett Packard 4284A LCR meter working in the frequency range from 20 to 10^6 Hz and with a 100 mV alternate signal. The spectra were collected at 298–473 K in different atmospheres, including dry air and wet air. In the latter case, the humidity content in the surrounding atmosphere was varied by bubbling air through liquid water at $T_W = 298$, 323 and 343 K, which should correspond to approximately 3, 12 and 31 kPa of water vapour pressure, respectively assuming equilibration between gas and liquid phases. The measurements were carried out on a day base with a fixed T_W value while the temperature of the sample, T_S, was increased from ca. 298 to 473 K (Fig. 1). After every modification of T_W, the sample was cooled down to room temperature and left over night (ca. 10 h) in dry air. The samples were equilibrated until steady-state conductivity values were attained. A thermocouple was placed as close as possible to the sample to obtain accurate temperature values. These values varied in a range from 2 to 3 K from sample to sample due to instability in the temperature control. The necessary electrical contacts on the samples were ensured by Pt porous electrodes pasted onto the surface of the ceramics and subsequently heated at 1073 K for 10 min.

Table 1
Sintering conditions and geometrical density of the ceramic samples (in the sample designations, D stands for dense and P for porous)

Sample	x	T_S (K)	t_S (h)	ρ (gcm^{-3})	Approximate grain size (μm)
NTZP20-P	2.0	1503	10	3.23	0.5–2.0
NTZP20-D	2.0	1493	40	3.31	0.5–1.5
NTZP22-P	2.2	1523	8	3.04	1.2–3.0
NTZP22-D	2.2	1538	8	3.22	2.0–4.0

3. Results and discussion

3.1. Microstructural and structural characterisation

Selected SEM micrographs typical for the studied ceramics are presented in Fig. 2. It can be seen that the highest densification is achieved for the $x = 2.0$ ceramics sintered at 1493 K during 40 h (NTZP20-D). The materials with $x = 2.2$ (NTZP22-D and NTZP22-P) exhibit a considerably larger number of pores, although sintered at higher temperatures (Table 1). The worse sinterability of NTZP22 composition has been previously reported[8] and may be explained by formation of a lower amount of liquid phase which is known to have an important role on the densification of NASICON ceramics. This liquid is thought to have a composition similar to Na_3PO_4.[9] Thus, the higher Na:P ratio for

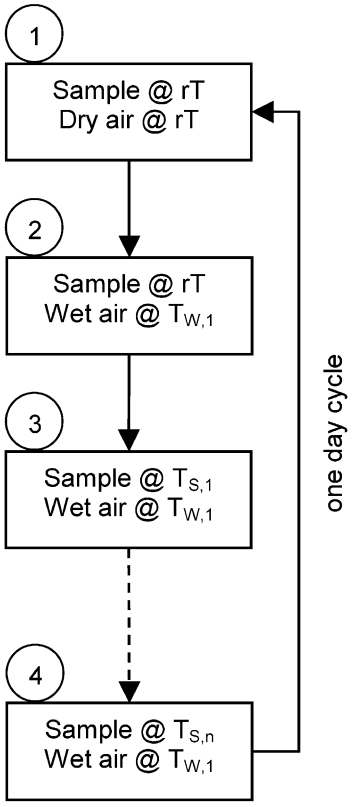

Fig. 1. Procedure for electrical measurements under different humidity conditions ($T_{S,i}$—temperature of the sample, $T_{W,i}$—temperature of the water bath used to obtain different moisture contents in the gas phase).

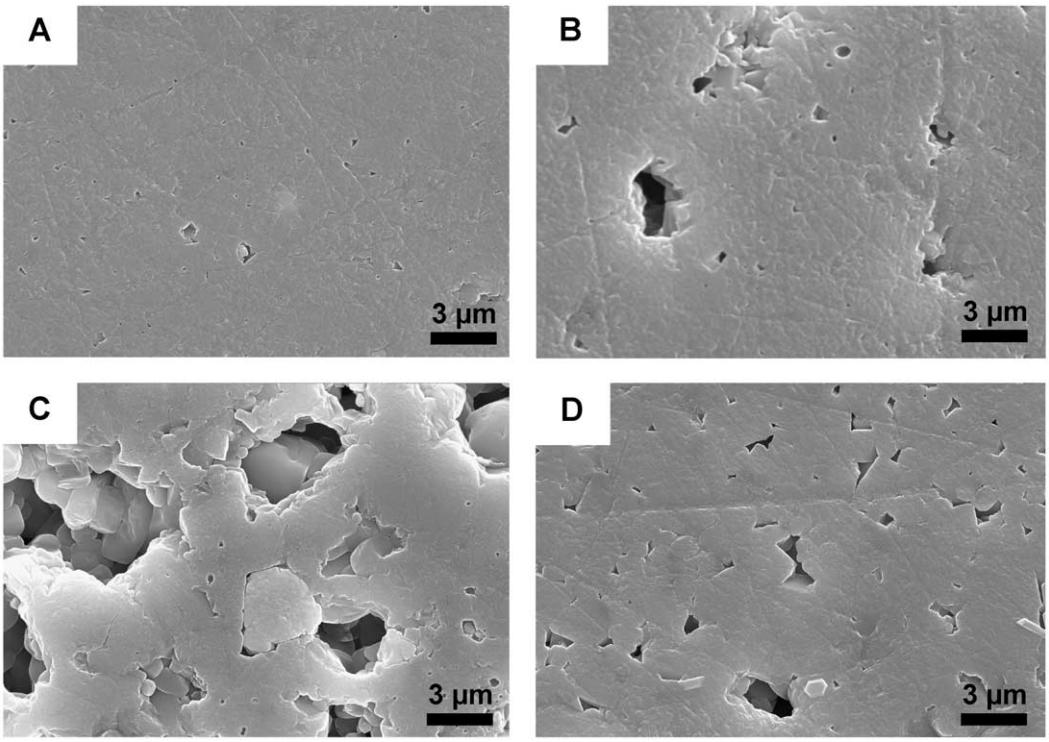

Fig. 2. SEM micrographs of (A) NTZP20-D, (B) NTZP20-P, (C) NTZP22-P and (D) NTZP22-D. All samples were polished and thermally etched at 1373 K for 30 min. See Table 1 for processing conditions.

NTZP22 is apparently resulting in smaller amount of liquid that hinders densification, when compared to materials with Na:P = 3:1. This is not surprising, since the Na_2O–SiO_2–P_2O_5 system phase diagrams show that the *liquidus* temperature decreases when increasing the fraction of P_2O_5.[15]

The analysis of NTZP20 samples etched at temperatures close to the sintering temperature (1458 K) revealed the presence of segregated zirconia grains appearing in lighter grey tonality (Fig. 3). Since these grains were not observed in the NTZP samples etched at 1373 K (Fig. 2A and B), it is reasonable to assume that zirconia is originally dispersed in the aforementioned liquid phase and precipitates during the high temperature etching. Contrary to NTZP20, Zr-enriched grains could not be observed in any of the analysed NTZP22 samples. The presence of significant fractions of monoclinic ZrO_2 ($mZrO_2$) in NTZP22 is, however, very likely if one compares the theoretical density predicted from XRD (ca. 3.28 gcm^{-3}) with the measured geometrical density (3.22 gcm^{-3}). Such high value of geometrical density (corresponding to about 98% densification) is not compatible with the apparent larger porosity of the samples evidenced by SEM (Fig. 2D). Due to relatively high density of $mZrO_2$ (5.41 gcm^{-3}) with respect to NASICON, and assuming simple mixture rules, the presence of 5 w.% of $mZrO_2$ in a hypothetic 90% pure dense NASICON sample would appear as a enhancement in density from about 2.95 to 3.22 gcm^{-3}. Moreover, the larger densities found for NTZP20 suggest higher fraction of $mZrO_2$ for this composition (Table 1).

In fact, the powder XRD patterns (Fig. 4) collected from ground ceramics show that not only NTZP20 but also NTZP22 is a mixture of NASICON and $mZrO_2$ as a second phase (arrowed peaks). Taking into account the diffraction intensities, the results further suggest that the fraction of $mZrO_2$ is higher for the NTZP20 samples, in agreement with the aforementioned deviation in reported densities. The same holds for the samples sintered at higher temperature, NTZP20-P and NTZP22-D. All patterns reveal the monoclinic symmetry of the NASICON lattice (space group C2/c) with unit cell parameters nearly independent of composition, in good agreement with previous work.[6]

3.2. *Effect of humidity on electrical conductivity at* $T \geqslant 373$ *K*

Fig. 5 shows impedance spectra of NASICON ceramics collected under different humidity conditions at 373 and 473 K. As expected for these relatively high temperatures and in this frequency range, the spectra reveal solely a pure ohmic resistance ascribed to the ceramic, R_t, and a capacitive tail due to the electrode process. While the values of R_t are only slightly affected by humidity, the electrode response clearly deviates from the capacitive behaviour expected for blocking Pt, air electrodes which is observed in dry air. Moreover,

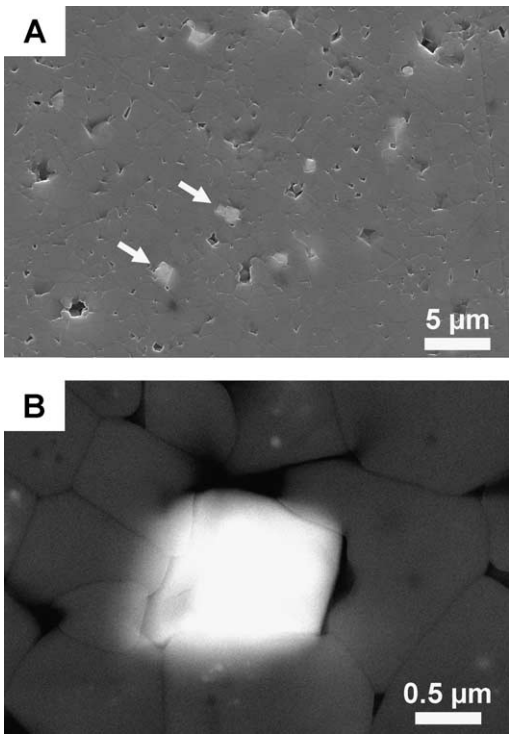

Fig. 3. SEM micrographs of a NTZP20-D ceramic sample polished and thermally etched at 1458 K for 30 min: (A) secondary electron image and (B) backscattered electron image showing a zirconia grain. Note the arrowed zirconia grains appearing in lighter tones.

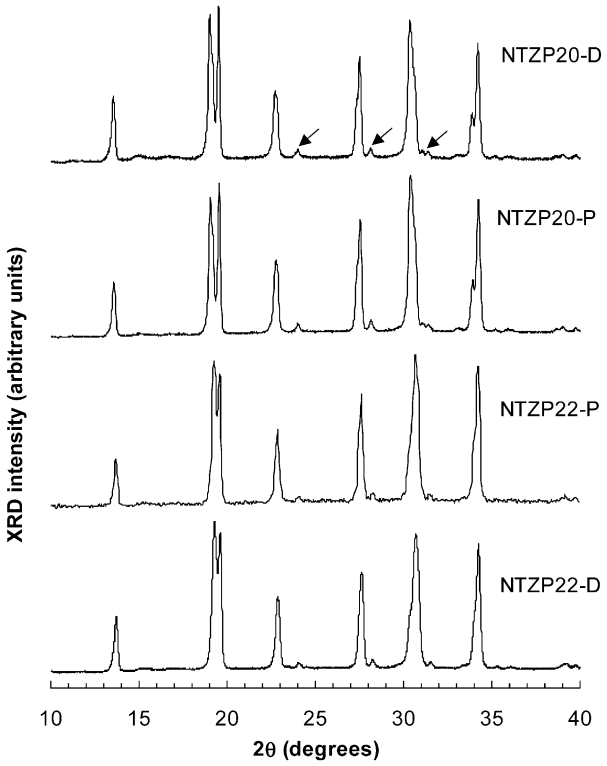

Fig. 4. XRD patterns collected on powdered ceramics samples (see Table 1 for processing conditions). The arrows point to the main monoclinic zirconia reflections indexed according to the JCPDS-ICDD card file no. 88-2390.

the effect of humidity is clearly more pronounced in the samples with higher porosity (NTZP22-D), in which a Warburg-like impedance is apparent at low frequency, and may be seen as a clear indication of the onset of some humidity-dependent process at the NASICON/Pt interface. The results, however, do not allow inferring any clear trend. Attempts to model the electrode response assuming different transmission line models suitable to account for variable capacitances were unsuccessful. This seems a rather complex problem and certainly implies the realisation of further experimental evidence obtained in future dedicated work. The evolution of the total resistance is, however, considerably more simple providing significant information.

The R_t values, taken as the high frequency intercept of the spectra, were thus used to obtain estimates of the total conductivity, σ_{tot}, in different temperature and humidity conditions. These values are shown in Fig. 6 using Arrhenius coordinates. It can be seen that the lowest σ_{tot} value was obtained with NTZP22-D, probably due to higher porosity (Fig. 2). It can also be seen that σ_{tot} decreases with increasing humidity at 423 and 473 K, while it decreases at 373 K. The latter effect is more pronounced for the porous NTZP22-P sample, suggesting that condensation of water vapour in the pores of both the ceramics and on the Pt electrodes may actually influence the electrode surface area as well as provide an alternative conductivity pathway along the continuous ceramics pores network. In fact, due to the adopted experimental procedure where samples are kept at room temperature while air humidity is increased, saturation of the gas phase occurs at temperatures higher than the first electrical measurements. In these conditions, water condensation is inevitable. Only above 373 K the sample temperature is always high enough to prevent condensation. However, even at 373 K, a deviation of 1–2 K between the sample temperature and the thermocouple reading is enough to allow for water condensation.

The release of combined and condensed water during the subsequent measurements at 423 and 473 K will probably favour additional degradation of the NASICON/Pt interface and the apparent decrease of σ_{tot} during condensation. A significant deterioration of the electrodes was indeed observed in all samples. This effect may be even stronger if secondary Na_3PO_4 phases are present at the grain boundaries or at the electrolyte/Pt electrode interface. It is well know that the tri-sodium phosphate easily forms hydrated (penta-, octa- or dodeca-hydrate) compounds at temperatures lower than about 323 K. Therefore, the temperature and pH_2O cycling may induce significant volume changes hence modifying the morphology of the interface. Possible errors in the estimation of small R_t values, typically of

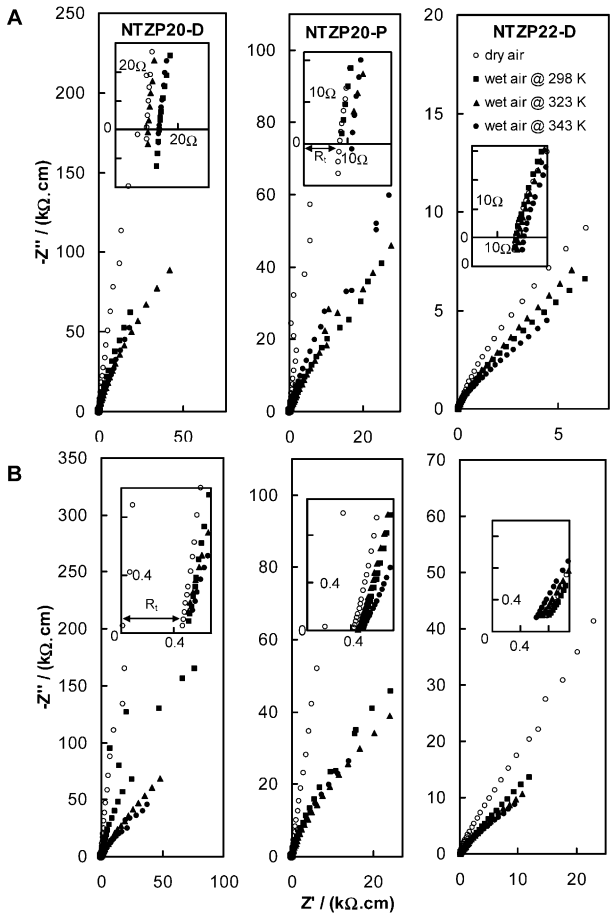

Fig. 5. Impedance spectra of different NASICON ceramics taken under different humidity conditions at approximately (A) 473 K and (B) 373 K. The insets show details of the high frequency part of the diagrams.

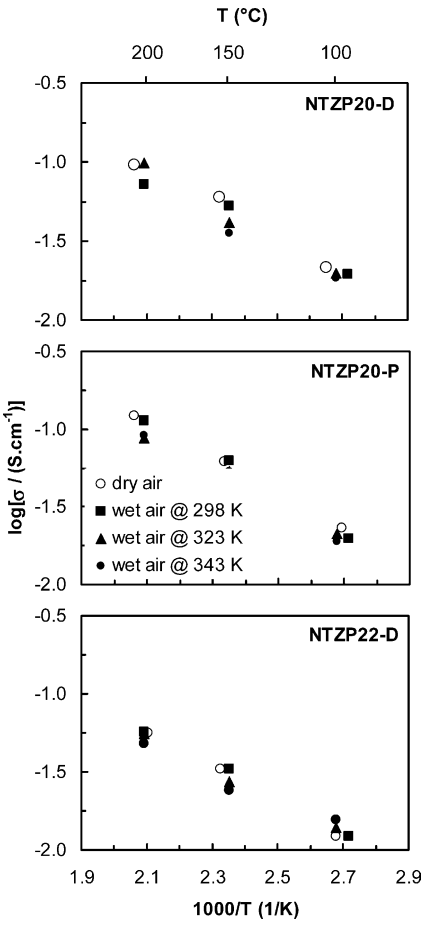

Fig. 6. Total conductivity of NASICON ceramics measured at different temperatures and humidities. The slight variation in the sample temperature results from different humidities.

the order of 20 and 10 Ω at 423 and 473 K, may also play a role, since, in these circumstances, the electrode impedance is comparatively much larger. This is particularly important in the cases where the real axis is not intercepted at high frequency (Fig. 5B) or the inductance due to the furnace electrical resistance clearly affects the spectra (Fig. 5A).

All in all, it may be concluded that the conductivity of NASICON is essentially independent of the water vapour pressure for the three ceramics, with an activation enthalpy of about 30 to 34 kJ/mol indicating that the conduction mechanism is the same in all materials, and under different moisture conditions. Notice that the activation enthalpy reported for NASICONs is close to 30 kJ/mol.

3.3. Low temperature impedance spectra

The experimental difficulties referred to in the previous section are a natural consequence of the instability of NASICON phases in contact with water, either liquid or vapour.[8–12] The effect of water condensation is particularly evident in the room temperature impedance spectra. The examples obtained with the NTZP20-P samples shown in Fig. 7 were selected to illustrate this effect. The spectra obtained under dry air have the expected shape consisting of a pure ohmic resistance due to the bulk impedance, a single slightly depressed semi-circle, which can be ascribed to the grain boundary impedance, and, at lower frequencies, the expected capacitive tale due to the Na^+-blocking NASICON|Pt, air interface. It can be seen that the amplitude of the grain boundary semicircle increases immediately after the first contact with the saturated atmosphere and decreases upon further increase of the saturation temperature and corresponding water condensation on the sample at lower temperatures. The effect of humidity in the electrode process is even stronger, showing an additional significantly depressed semicircle that clearly deviates from the capacitive behaviour observed in dry air. Moreover, the initial spectra obtained with fresh sample and electrodes could not be obtained on subsequent measurements in dry air (Fig. 8, spectra b and c). These were approximately recovered only after

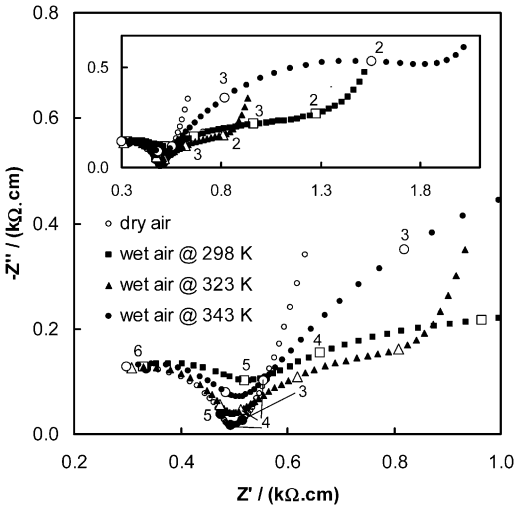

Fig. 7. Impedance spectra of NTZP20-P taken at room temperature under different humidity conditions. Numbers indicate the $\log_{10}$ of the frequency.

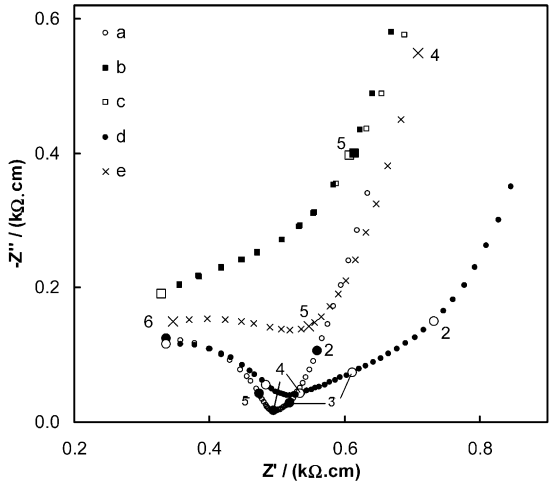

Fig. 8. Room-temperature impedance spectra of a NTZP20-P ceramic collected in dry air after exposing to different humidity conditions. The measurements were collected in the sequence shown in the legend: (a) fresh sample and electrodes; (b) after measuring at $T_W = 298$ K; (c) after a series of measurements with $T_W = 298$, 323 and 343 K; (d) after polishing and deposition of fresh electrodes; (e) after a final series of measurements with $T_W = 298$, 323 and 343 K. Numbers indicate the $\log_{10}$ of the frequency.

careful polishing of the electrolyte surface and deposition of new electrodes (spectrum d). Although to a smaller extent, the irreversible modification of the spectra is again observed after a new series of measurements under saturated atmospheres (spectrum e).

The onset of the additional electrode component is thus clearly resulting from the water condensed over the NASICON and electrode surfaces creating additional electrochemical interfaces, which are likely contributors to the overall electrode response. The electrochemical response of these interfaces may explain the unexpected non-blocking behaviour of the NASICON/Pt, air electrodes and its dependence on humidity. Such processes may include the dissolution of amorphous material from the grain boundaries causing the deterioration of the NASICON/Pt electrode contact and the increase of the grain boundary impedance. Formation of the so called hydronium-NASICON[13] demands considerably larger reaction times,[11,12] and seems unlikely in this case. It is perhaps interesting to note that previously reported non-blocking electrodes in Pt/NASICON/Pt cells[16,17] may thus be related to the presence of water at the ceramic and metal electrode surfaces, or at the ceramic/electrode interfaces. Although still a possibility, the existence of protonic conduction at temperatures lower than 373 K remains difficult to confirm. In fact, and as for higher temperatures, the values of total conductivity are similar for all samples whereas the activation enthalpies estimated from room temperature up to 473 K all fall in the same range estimated between 273 and 473 K.

4. Conclusions

NASICON-type powders with nominal composition $Na_3Si_2Zr_{1.88}Y_{0.12}PO_{11.94}$ and $Na_{3.2}Si_{2.2}Zr_{1.88}Y_{0.12}P_{0.8}O_{11.94}$ were prepared by a standard solid-state synthesis route using a reactive zirconia precursor. These powders were used to obtain ceramic samples with different microstructures. X-ray diffraction and scanning electron microscopy analysis of materials processed under different conditions suggested that the amount of Na- and P-rich liquid phases formed during the high temperature sintering is smaller for $Na_{3.2}Si_{2.2}Zr_{1.88}Y_{0.12}P_{0.8}O_{11.94}$. Indeed, samples of this composition showed a considerably worse sinterability.

In spite of the difficulties experienced during the conductivity measurements in wet atmospheres, results obtained at temperatures between 373 and 473 K show no evidence for protonic conduction in NASICON. Results obtained at lower temperatures were not conclusive to this respect perhaps due the instability of the material and the electrodes in contact with condensed water.

Acknowledgements

This work was supported by the FCT, Portugal. O. Smirnova is funded by FCT (grant BD/6594/2001).

References

1. Hong, H. Y. P., Crystal structures and crystal chemistry in the system $Na_{1+x}Zr_2Si_xP_{3-x}O_{12}$. *Mat. Res. Bull.*, 1976, **11**, 173–182.
2. Goodenough, J. B., Hong, H. Y. P. and Kafalas, J. A., Fast Na^+-ion transport in skeleton structures. *Mat. Res. Bull.*, 1976, **11**, 203–220.

3. Ahmad, A., Glasgow, C. and Wheat, T. A., Sol-gel processing of NASICON thin-film precursors. *Solid State Ionics*, 1995, **76**, 143–154.
4. Kida, T., Miyachi, Y., Shimanoe, K. and Yamazoe, N., NASICON thick film-based CO_2 sensor prepared by a sol-gel method. *Sensors and Actuators B*, 2001, **80**, 28–32.
5. Caneiro, A., Fabry, P., Khireddine, H. and Siebert, E., Performance characteristics of a sodium super ionic conductor prepared by sol-gel route for sodium ion sensors. *Anal. Chem.*, 1991, **63**, 2550–2557.
6. Khireddine, H., Fabry, P., Caneiro, A. and Bochu, B., Optimization of NASICON composition for Na^+ recognition. *Sensors and Actuators B*, 1997, **40**, 223–230.
7. Boilot, J. P., Salaine, J. P., Desplanches, G. and Le Potier, D., Phase transformations in $Na_{1+x}Si_xZr_2P_{3-x}O_{12}$ compounds. *Mater. Res. Bull.*, 1979, **14**, 1469–1477.
8. Ahmad, A., Wheat, T. A., Kuriakose, A. K., Canaday, J. D. and McDonald, A. G., Dependence of the properties of NASICONS on their composition and processing. *Solid State Ionics*, 1987, **24**, 89–97.
9. Mauvy, F., Siebert, E. and Fabry, P., Reactivity of NASICON with water and interpretation of the detection limit of a NASICON based Na^+ ion selective electrode. *Talanta*, 1999, **48**, 293–303.
10. Kida, T., Shimanoe, K., Miura, N. and Yamazoe, N., Stability of NASICON-based CO_2 sensor under humid conditions at low temperature. *Sensors and Actuators B*, 2001, **75**, 179–187.
11. Fuentes, R. O., Figueiredo, F. M., Marques, F. M. B. and Franco, J. I., Reaction of NASICON with water. *Solid State Ionics*, 2001, **139**, 309–314.
12. Gulens, J., Hildebrandt, B., Canaday, J., Kuriakose, Wheat, T. A. and Ahmad, A., Influence of water on the electrochemical response of a bonded NASICON protonic conductor. *Solid State Ionics*, 1989, **35**, 45–49.
13. Komorowski, P. G., Argyropoulos, S. A., Hancock, R. G. V., Gulens, J., Taylor, P., Canaday, J. D., Kuriakose, A. K., Wheat, T. A. and Ahmad, A., Characterization of protonically exchanged NASICON. *Solid State Ionics*, 1991, **48**, 295–301.
14. Yagi, H. and Saiki, T., Humidity sensor using NASICON not containing phosphorus. *Sensors and Actuators B*, 1991, **5**, 135–138.
15. Phase Diagrams for Ceramists, figs. 535-537, American Chemical Society, Columbus, 1964.
16. Dygas, J. R., Fafilek, G. and Breiter, M. W., Study of grain boundary polarization by two-probe and four-probe impedance spectroscopy. *Solid State Ionics*, 1999, **119**, 115–125.
17. Pasierb, P., Komornicki, S., Gajerski, R., Koziński, S., Tomczykand, P. and Rekas, M., Electrochemical gas sensor materials studied by impedance spectroscopy Part I: NASICON as solid electrolyte. *J. Electroceramics*, 2002, **8**, 49–55.